Available online at www.sciencedirect.com
ScienceDirect
Catalysis Today 130 (2008) 354–360
CATALYSIS TODAY
www.elsevier.com/locate/cattod

Cyclohexene hydrogenation with molybdenum disulfide catalysts prepared by *ex situ* decomposition of ammonium thiomolybdate-cetyltrimethylammonium thiomolybdate mixtures

R. Romero-Rivera [a], M. Del Valle [a], G. Alonso [b], E. Flores [c], F. Castillón [c], S. Fuentes [c], J. Cruz-Reyes [a,*]

[a] *Facultad de Ciencias Químicas e Ingeniería, Universidad Autónoma de Baja California, Tijuana, B.C., Mexico*
[b] *Depto de Catálisis, Centro de Investigación en Materiales Avanzados, Chihuahua, Chih., Mexico*
[c] *Centro de Ciencias de la Materia Condensada, Universidad Nacional Autónoma de México, Ensenada, B.C., Mexico*

Available online 3 December 2007

Abstract

Ammonium tetrathiomolybdate (ATTM) is treated with cetyltrimethylammonium chloride (CTAC) using several ATTM/CTAC ratios. Reaction of ATTM with the limiting reagent CTAC gives the carbon-containing compound cetyltrimethylammonium tetrathio-molybdate (CTAT), resulting in different ATTM–CTAT mixtures or precursors which are then decomposed in N_2 at 723 K, yielding mesoporous samples with surface areas of over 260 m^2/g. Analysis by XRD and electron microscopy correspond to a well dispersed MoS_2–2H phase. The activity of the catalysts is tested in a batch reactor for cyclohexene hydrogenation, where those prepared from ATTM–CTAT precursors are up to seven times more active than the catalyst obtained by thermal decomposition of pure ATTM. The enhanced catalytic activity of these catalysts is attributed to a sulfide phase containing structural carbon.

Keywords: High-surface area MoS_2; Hydrogenation; Cyclohexene; Cetyltrimethylammonium chloride

1. Introduction

The use of transition metal sulfide (TMS) catalysts in oil refinery hydrotreating has helped reduce the toxic SOx and NOx atmospheric emissions of internal combustion engines for several decades. Hydrotreating catalysis involves a variety of reactions, among them, hydrodesulfurization (HDS), hydrodenitrogenation, hydrodeoxygenation, and hydrogenation [1–4].

Several methods are used to prepare sulfide catalysts: sulfidation of coprecipitated oxides [5,6] comaceration [7,8], homogeneous sulfide precipitation [9], ceramic method [10], impregnated thiosalt decomposition [11], all of which yield compounds with surface areas in the order of 5–50 m^2/g.

Tetraalkylammonium thiometallates have been synthesized by the metathesis reaction between ammonium tetrathiomolybdate with tetraalkylammonium chlorides [12] or tetraalkylammonium hydroxides using acetonitrile as a solvent [13]. Transition metal sulfide precursors $(NR_4)_2MS_4$, where R=H, CH_3, or C_4H_9 (alkyl group) and M=Mo or W, were prepared by reacting ammonium tetrathiomolybdate with the corresponding tetraalkylammonium bromide in an aqueous medium, followed by *in situ* decomposition [14,15].

The *in situ* decomposition of tetraalkylammonium thiomolybdates yields molybdenum sulfide catalysts with high-surface area and improved catalytic properties in the HDS of dibenzothiophene. This behavior has been associated with the presence of carbon in substitution of sulfur atoms, generating systems like $MoS_{2-x}C_x$ [16]. In the synthesis of ruthenium sulfides carbon content has also been observed according to the formula: $RuS_{2-x}C_x$ [17,18]. Greater excess of sulfur in Ru and Mo sulfide catalysts with general formula MS_{2+x} as been found to yield a greater carbon content $MoS_{2-x}C_x$ after HDS in organic solvents [19]. On the other hand, researchers have found that metal sulfides supported on carbon show a much greater activity than the same sulfides when supported in alumina [20,21].

* Corresponding author. Tel.: +52 664 6822790.
E-mail address: juancruz@uabc.mx (J. Cruz-Reyes).

0920-5861/$ – see front matter
doi:10.1016/j.cattod.2007.10.099

Highly dispersed molybdenum sulfides have recently been produced from precursors obtained by treating aqueous ATTM with CTAC and reducing agents like hydroxylamine sulfate or hydrazine hydrate [22], resulting in surface areas of up to 211 m^2/g. In recent work [23], the treatment of ATTM using an ATTM/CTAC ratio (1/0.2) gives precursors that yield MoS_2 catalysts with similar surface areas.

This work studies the properties of MoS_2 catalysts obtained from the thermal decomposition of precursors resulting from ATTM treated with different quantities of CTAC (ATTM/CTAC molar ratio = 2.5–0.5) including the evaluation of their catalytic activity for the model cyclohexene hydrogenation.

2. Experimental

2.1. Preparation of molybdenum sulfide precursors (MSP)

Untreated $(NH_4)_2MoS_4$, the molybdenum sulfide precursor MSP1, was prepared according to the method described by Berhault [24] which requires adding $(NH_4)S$, 42.5% in aqueous solution to $(NH_4)_6[Mo_7O_{24}]_4{\cdot}H_2O$ diluted in a minimum amount of water to produce a dark red crystalline precipitate.

Precursor MSP2 was prepared by dissolving 1.0 g (3.84 mmol) $(NH_4)_2MoS_4$ in water (30 mL) and adding 1.56 mmol CTAC as a 25% aqueous solution (2 mL) and stirring for 1 h at room temperature. The resulting precipitate was isolated by vacuum filtration, and kept under N_2 atmosphere. Precursors MSP3, MSP4, MSP5, MSP6 were prepared in a similar way as MSP2, using 4, 6, 8 and 10 mL of CTAC 25% aqueous solution, respectively, to treat MSP.

2.2. Preparation of molybdenum sulfide catalysts (MSC)

The molybdenum sulfide catalysts were prepared by grinding 1.0 g of each precursor, placing it in a porcelain boat, introducing it in the alumina tube of a tubular furnace with N_2 gas flow, increasing temperature to 723 K (10 K/min heating rate) and then kept constant for 2 h. The furnace was later allowed to cool to 473 K and immediately after, the gas flow was cut and the system was allowed to cool down to room temperature. Finally, the sample was kept under N_2 atmosphere.

2.3. Characterization of samples

Horizontal attenuated total reflectance (HATR) IR spectroscopy was recorded with a Series 1700 Perkin-Elmer FTIR spectrophotometer. The IR sample was ground in an agatha mortar and placed evenly on the HATR device.

Specific surface area was measured with a Quantachrome AUTOSORB-1 by N_2 absorption at 77 K using the BET isotherm and a sample mass of 0.2–0.3 g. Samples were degassed under flowing argon at 473 K for 2 h before N_2 adsorption. The pore size distribution was obtained from the desorption data, following the BJH method. The mean standard deviation for the surface area measurements was about 2%.

The X-ray diffraction patterns of the prepared samples were obtained with a Philips X'Pert analytical diffractometer for powder samples using Cu Kα radiation. Their phases were identified with reference to the database of the International Centre for Diffraction Data.

A Jeol JSM5800 IV scanning electron microscope was used to perform morphology and EDX elemental analysis. Several fields were analyzed at different magnifications in order to recognize the prevalent features. EDX analysis was performed using an eBX-ZAF system, using an MoS_2 reference sample to deconvolute the L lines of S and Mo. Transmission electron microscopy was done on a Philips FEG TECNAI F20 transmission electron microscope operated at 200 kV.

2.4. Catalytic activity

The catalytic activity for cyclohexene hydrogenation was tested in a high-pressure 300 mL Parr reactor by placing 20 mL of cyclohexene with 0.3 g of catalyst. The reactor was purged of residual air, pressurized with H_2 to 35.91 kPa (750 psi) then heated to the reaction temperature of 543 K in about 10 min. A stirring rate of 50 rpm was used. The advance of the reaction was monitored by GC using samples taken every 20 min during the first hour, then every 30 min for the next 4 h. Reduction of sample volume due to sampling was $\leq$5% of total volume. Catalytic function was expressed in terms of % conversion of cyclohexene versus time and from these data, initial reaction rates were calculated for each catalyst.

2.5. Gas chromatography

Samples obtained from the reactor were analyzed using a Hewlett–Packard 6890 gas chromatograph with FID detector. A low polarity J&W DB624 capillary column, 30 m long, 0.53 mm diameter, 3.0 μm thick liquid phase was employed. Column temperature was 373 K, using a N_2 carrier gas flow of 3 mL/min and a split ratio of 1:10.

3. Results and discussion

3.1. Infrared spectroscopy

Reflectance FT-IR spectral data in the 465–485 cm^{-1} region is presented in Fig. 1 and Table 1. For precursor MSP1 (pure ATTM), a single absorption band is observed around 467 cm^{-1} which is assigned to the Mo–S stretching vibration. This band becomes considerably weaker for the MSP2 sample and is barely visible in the spectra of the remaining samples in the series. Precursor MSP6 (from the stoichiometric reaction between ATTM and CTAC) presents a single absorption band at 477.19 cm^{-1}, which is assigned to the Mo–S stretching vibration of CTAT, in close agreement with the corresponding absorption bands previously reported for other alkylammonium thiomolybdates [25]. For precursors MSP2 through MSP5 a clear displacement of the CTAT absorption band from 476.10 to 477.99 cm^{-1} is observed. This effect has been attributed to solid-state cation–anion interactions between the unreacted ATTM and the CTAT product in the precursor mixtures [26].

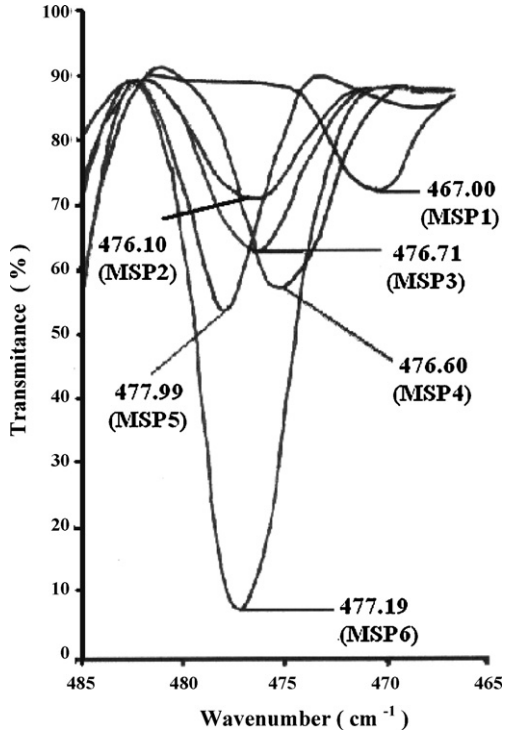

Fig. 1. Far FTIR spectra of prepared MSP catalyst precursors.

From these results it is proposed that a metathesis reaction between ATTM and the limiting reagent CTAC produces the carbon-containing compound cetyltrimethylammonium tetrathiomolybdate (CTAT), according to

$$(NH_4)_2MoS_4 + 2CH_3(CH_2)_{15}N(CH_3)_3Cl \rightarrow [CH_3(CH_2)_{15}N(CH_3)_3]_2MoS_4 + 2NH_4Cl$$

Since all precursor preparations except MSP1 use more than the stoichometric 1:2 ratio of ATTM/CTAC, the excess ATTM in the product results in different ATTM–CTAT mixtures or precursors.

3.2. X-ray diffraction

The diffraction patterns of the prepared MoS_2 catalysts are compared in Fig. 2. While the samples obtained by thermal decomposition are all microcrystalline, the pattern for the MSC1 sample, Fig. 2(a), is composed of several broad peaks, corresponding to the (0 0 2), (1 0 0), (1 0 3), (1 1 0) and (0 0 8) reflections reported for the structure of poorly crystalline

Table 1
Infrared spectral data for MoS_2 catalyst precursors

Precursor	IR wavenumbers (cm^{-1})
MSP1	467.00
MSP2	476.10
MSP3	476.71
MSP4	476.60
MSP5	477.99
MSP6	477.19

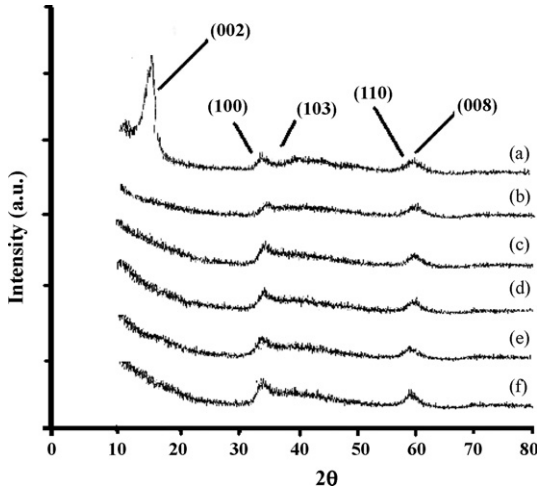

Fig. 2. XRD patterns of the prepared MoS_2 catalysts: (a) MSC1, (b) MSC2, (c) MSC3, (d) MSC4, (e) MSC5, and (f) MSC6.

MoS_2–2H [25,27]. The broad peaks indicate a microcrystalline, nearly amorphous material. However, the peak at $2\theta = 14^\circ$ corresponds to the well-defined (0 0 2) reflection of MoS_2–2H, which implies a significant amount of basal layer stacking in the "*c*" direction of the catalyst particles. The reflection corresponding to the (1 0 0) is less intense than in MoS_2–2H crystals and the (1 0 3) planes are absent. The asymmetric form of the (1 0 0) family is a characteristic of random layered structures [28,29].

The XRD patterns shown in Fig. 2(b)–(f) belong to the catalyst materials obtained by decomposition of MSP treated with different amounts of CTAC, including the stoichometric 1:2 ratio. Analysis of these patterns identifies the (1 0 0), (1 0 3), and (1 1 0) reflections of MoS_2–2H. The absence of the (0 0 2) reflection suggests high dispersion due to crystallites of only a few atomic layers, attributed to the presence of carbon derived from the decomposition of CTAT in a way analogous to the high dispersion of MoS_2 reported by others for carbon-supported MoS_2 catalysts [20,21]. Similar XRD patterns have been obtained for chemically exfoliated MoS_2 and WS_2 catalysts [30,31].

3.3. Elemental analysis

The EDX analysis for all prepared molybdenum disulfide catalysts are reported in Table 2. The S/Mo atomic ratio for all

Table 2
Specific surface area, total pore volume and atomic ratios determined from elemental analysis by EDX for prepared MoS_2 catalysts

Catalyst	Surface area (m^2/g)	Total pore volume (cm^3/g)	Mo	S/Mo	C/Mo
MSC1	5	0.04	1	2.10	–
MSC2	154	0.13	1	1.92	5.02
MSC3	188	0.16	1	1.95	10.00
MSC4	186	0.17	1	2.18	10.69
MSC5	267	0.17	1	2.25	9.30
MSC6	104	0.16	1	1.85	9.67

samples is around 2 (1.85–2.25), which is consistent with the MoS_2 phase. High amounts of carbon ($5.02 \leq C/Mo \leq 10.69$) are found in all the MoS_2 catalysts, except for the one obtained from untreated ATTM. This carbon is considered to be adsorbed on the surface of the sulfide, rather than structural in nature. Also, in contrast to sulfur deficient sulfide catalysts obtained from *in situ* decomposition of precursors during HDS of DBT, the MSC series of catalysts are not sulfur deficient.

3.4. Surface area and pore size distribution

Table 2 lists the surface area values and the total pore volume for MoS_2 catalysts produced by thermal decomposition of the precursor series. The surface area of the catalysts increases as the amount of CTAT in the corresponding precursor increases, reaching a maximum value for MSC5, then decreases for the catalyst MSC6 derived from ATTM treated with a stoichiometric (1:2) amount of CTAC. Even a small amount of CTAT, as evidenced by the MSC2 sample in Table 2, results in a marked increase in MoS_2 surface area. Other authors have also found that MoS_2 derived from different treatments with CTAC present higher surface areas than those prepared by thermal decomposition of pure ATTM [32].

It is assumed that as the amount of the carbon-containing CTAT gradually increases in the precursor mix, so does the amount of carbon that – upon decomposition of CTAT – is adsorbed by the MoS_2 phase; however, when the composition of the precursor that yields MSC6 is reached, the excess carbon probably begins to deposit on the active surface of the molybdenum sulfide, and the surface area begins to significantly decrease compared to that of the prior ATTM–CTAT precursors. Thermal decomposition of pure ATTM in a mixture of H_2S/H_2 generally yields moderate surface areas in the order of 10–50 m^2/g [27,33], attributed to particle sintering, whereas *in situ* thermal decomposition of ATTM produces high-surface area molybdenum sulfides [16].

According to Table 2, the carbon content of the MoS_2 precursor has an important effect on the surface area and the total pore volume of the catalysts. Carbon-containing catalysts MSC2–MSC6, show surface areas 20–30 times greater than that of MSC1 (5 m^2/g), obtained from pure ATTM, while total pore volume is three to four times greater than that of MSC1 (0.04 cm^3/g). Similar pore volume distributions, centered on different pore sizes have been reported for MoS_2 catalysts obtained from other alkyl-thiosalts [34].

The adsorption isotherms and pore volume distributions for the prepared catalysts are shown in Figs. 3 and 4, respectively. All catalysts exhibit a Type IV isotherm. The MSC1 catalyst prepared from pure ATTM has a poorly developed porous system which results in its low surface area. The MSC2–MSC6 catalysts have better developed porous systems, with an average pore diameter of around 35 Å (Fig. 4). The hysteresis loop of MSC2 appears to be less developed and has a narrower pore size distribution than MSC3–MSC6. The MSC6 catalyst has the widest hysteresis loop and broadest pore size distribution, which includes larger pore diameters. The hysteresis loops shown by these catalysts correspond mainly to cylindrical pores open at both ends.

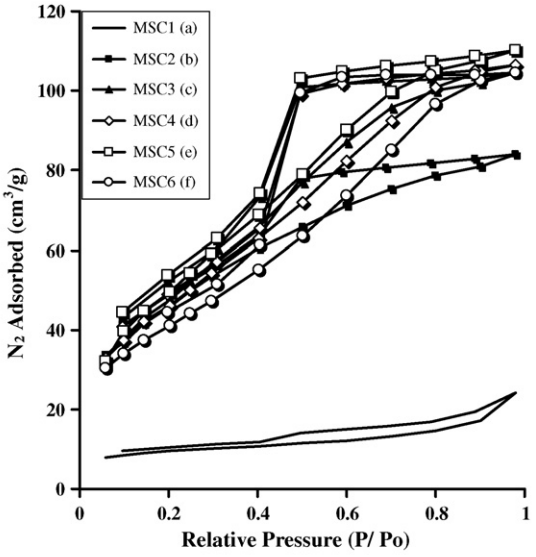

Fig. 3. Adsorption–desorption isotherms of the prepared MoS_2 catalysts: (a) MSC1, (b) MSC2, (c) MSC3, (d) MSC4, (e) MSC5, and (f) MSC6.

3.5. Electron microscopy

SEM micrographs of the prepared MoS_2 catalysts are reported in Fig. 5. With the exception of MSC1, all the solids appear very porous with cavities probably resulting from the elimination of gas products during the course of the thermal decomposition process. For MSC1 relatively few cavities are observed, in agreement with the porosimetry data for a poorly developed porous organization.

The disordered microstructure of the MoS_2 catalysts is seen in the TEM micrographs presented in Fig. 6, where the layer

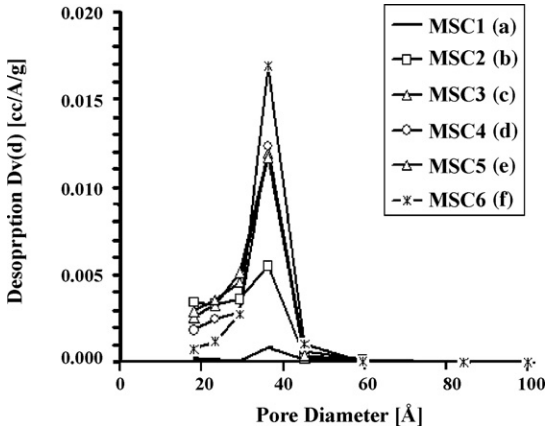

Fig. 4. BJH pore size distribution of the prepared MoS_2 catalysts: (a) MSC1, (b) MSC2, (c) MSC3, (d) MSC4, (e) MSC5, and (f) MSC6.

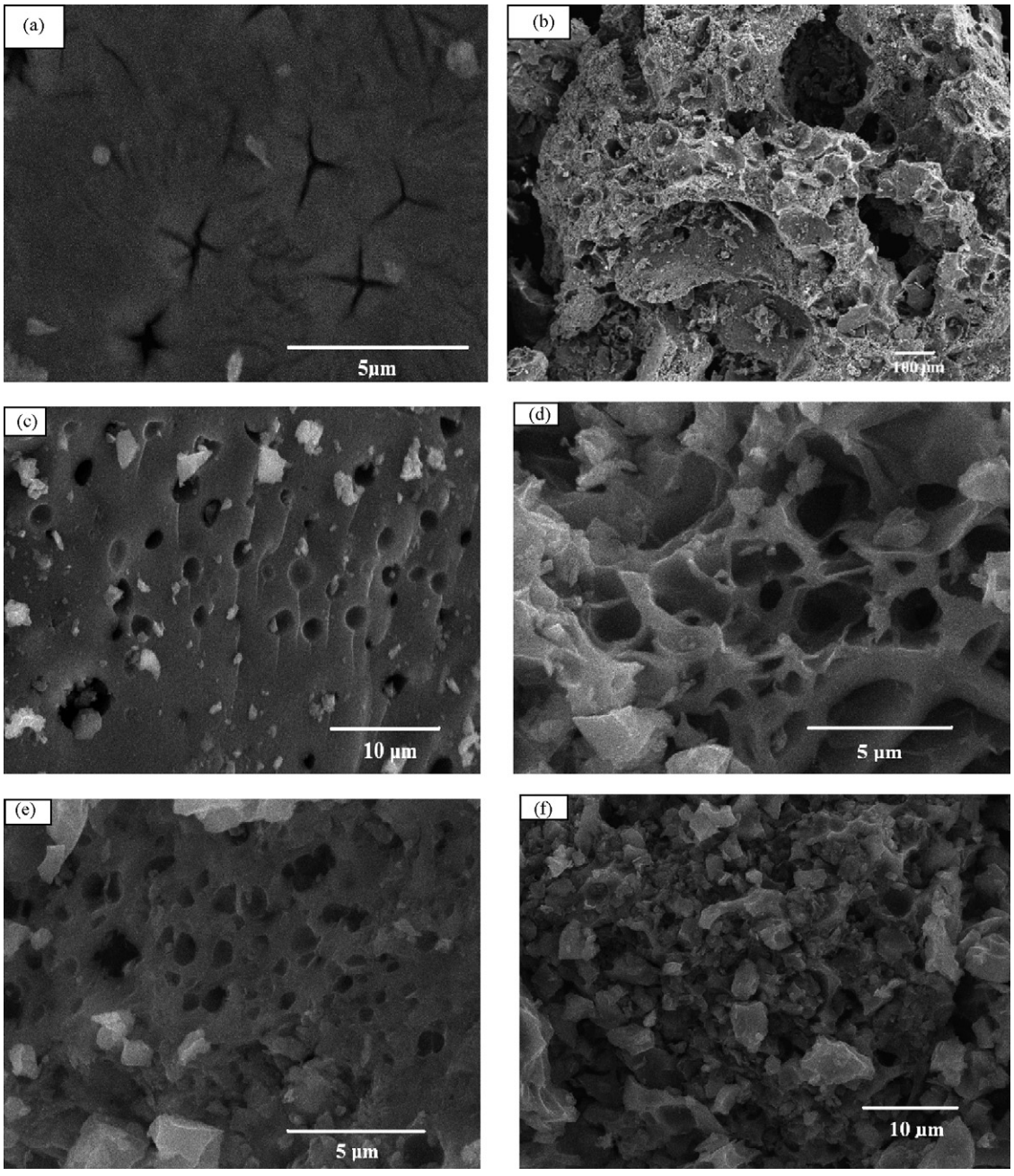

Fig. 5. Scanning electron micrographs of the prepared MoS_2 catalysts: (a) MSC1, (b) MSC2, (c) MSC3, (d) MSC4, (e) MSC5, and (f) MSC6.

spacing corresponds to MoS_2 (0 0 2) plane stacking [35]. On average, catalysts MSC2–MSC6 show a lesser degree of layer stacking (Fig. 6b) than catalyst MSC1, obtained from pure ATTM (Fig. 6a).

3.6. Catalytic activity

Analysis of the kinetic data by the integration method finds that the hydrogenation reaction closely follows a first-order reaction law over the 5 h reaction time. The cyclohexene conversions after 5 h for the MSC1 and MSC6 catalysts are nearly the same (around 34%), which means that the precursor consisting of CTAT, compared to ATTM, does not give a higher activity MoS_2 catalyst. In contrast, conversions of up to 90% are found for MoS_2 catalysts obtained from precursors containing some amount of ATTM. Kinetic data for all the catalysts are consigned in Table 3, along with Figs. 7 and 8. While the initial reaction rate ratio between MSC6 and MSC1 is 1.04 the rate ratio between MSC4 and MSC1 is seven times greater. The increase is attributed to the greater dispersion of the catalysts induced by the presence of carbon and perhaps organic matter derived from the decomposition of the ATTM–CTAT precursors, while the MSP6 precursor may generate enough surface carbon in MSC6 to counter the increased activity of the catalyst. The initial reaction rate for MSC1 is of the same order of magnitude than those reported for a similar system [23] and a

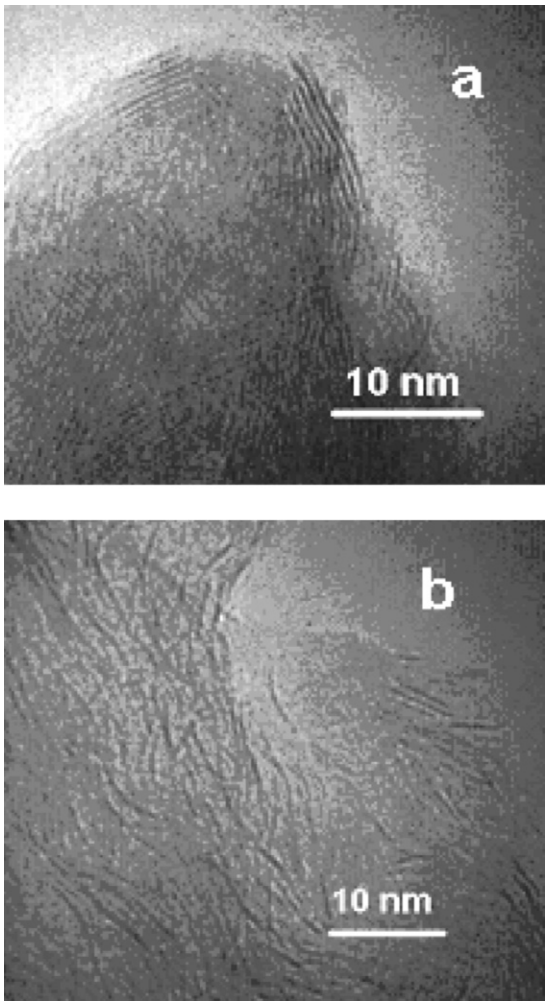

Fig. 6. TEM micrographs of MoS_2 catalysts: (a) MSC1 and (b) MSC6.

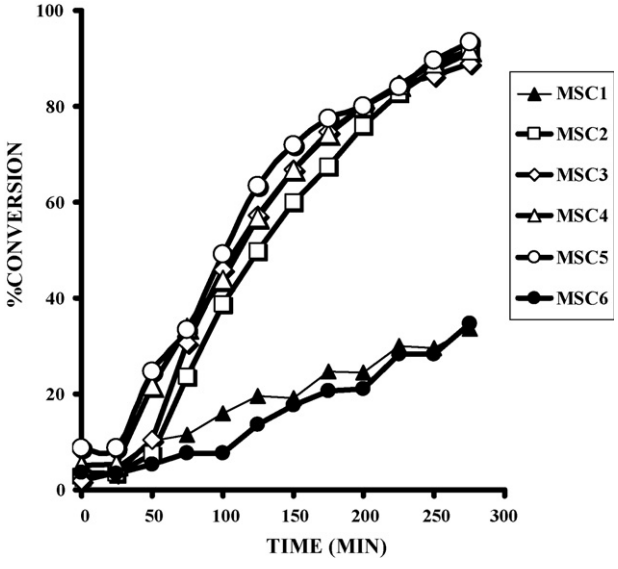

Fig. 7. Plot of conversion vs. time for cyclohexene hydrogenation, for the series of MSC catalysts.

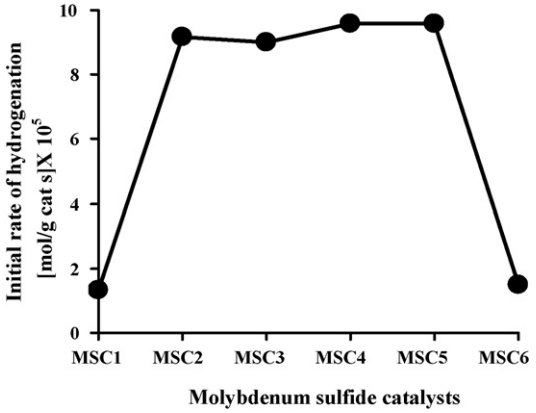

Fig. 8. Plot of initial rates of hydrogenation for the series of MSC catalysts.

Table 3
Kinetic data for the prepared MoS_2 catalysts

Catalyst	Conversion (%)	k ($\times 10^5$ s^{-1})	Initial reaction rate ($\times 10^5$ mol/g cat s)
MSC1	33.7	2.0	1.3
MSC2	91.2	14.0	9.2
MSC3	88.8	13.8	9.0
MSC4	91.6	14.7	9.6
MSC5	93.5	14.7	9.6
MSC6	34.5	2.3	1.5

Mo/Al_2O_3 catalyst [36], both for the hydrogenation of cyclohexene. No recognizable trend between BET surface area and catalytic activity is found, as is often the case for sulfide catalysts in general [1].

4. Conclusions

The thermal decomposition of ATTM–CTAT mixtures or precursors, as well as pure CTAT, yields high-surface area MoS_2 catalysts, compared to that obtained from pure ATTM. Surface areas are comparable to those reported in the literature for MoS_2 catalysts obtained using a 1:1 ratio of ATTM/CTAC meaning the 1:1 ratio is not critical to attaining high-surface areas.

The XRD patterns of the MSC2–MSC6 samples correspond to poorly crystalline MoS_2. The absence of the (0 0 2) reflection indicates that these MoS_2 catalysts are highly dispersed materials. Electron microscopy analysis is consistent with the XRD results.

The use of ATTM–CTAT mixtures as MoS_2 precursors, when thermally decomposed, produce catalysts having a seven-times greater rate constant than the catalyst derived from pure ATTM, for the cyclohexene hydrogenation.

Acknowledgements

We gratefully acknowledge the XRD technical assistance of Eloisa Aparicio (CCMC-UNAM), Carlos Ornelas and Francisco Paraguay (CIMAV). We also acknowledge the support of CONACYT under Grants no. 53087 and 55490.

References

[1] O. Weisser, Landa, Sulfide Catalysts: Their Properties and Applications, Pergamon Press, Oxford, 1973.
[2] P. Grange, Catal. Rev. Sci. Eng. 21 (1980) 135.
[3] M. Zdrazil, Catal. Today 3 (1988) 269.
[4] H. Topsoe, B.S. Clausen, F.E. Massoth, Hydrotreating Catalysis, Science and Technology, Springer-Verlag, Germany, 1996, p. 11.
[5] K.C. Pratt, J.V. Sanders, N. Tamp, J. Catal. 23 (1971) 205.
[6] J.V. Sanders, K.C. Pratt, J. Catal. 67 (1981) 331.
[7] G. Hagenbach, Ph. Courty, B. Delmon, J. Catal. 23 (1971) 295.
[8] G. Hagenbach, Ph. Courty, B. Delmon, J. Catal. 31 (1973) 264.
[9] R. Candia, B.J. Clausen, H. Topsoe, Bull. Soc. Chim. Belg. 90 (1981) 1225.
[10] A.A. Hilli-al, B.L. Evans, J. Cryst. Growth 15 (1972) 93.
[11] S. Fuentes, G. Díaz, F. Pedroza, H. Rojas, N. Rosas, J. Catal. 113 (1988) 535.
[12] T.E. Wolff, J.M. Berg, K.O. Hodgson, R.B. Frankel, R.H. Holm, J. Am. Chem. Soc. 101 (1979) 4140.
[13] W.J.W. McDonald, G. Delbert Friesen, L.D. Rosehein, W.E. Newton, Inorg. Chem. Acta 72 (1983) 205.
[14] G. Alonso, M. Del Valle, J. Cruz, V. Petranovskii, A. Licea-Claverie, S. Fuentes, Catal. Today 43 (1998) 117.
[15] G. Alonso, V. Petranovskii, M. Del Valle, J. Cruz-Reyes, A. Licea-Claverie, S. Fuentes, Appl. Catal. A: Gen. 197 (2000) 87.
[16] R.R. Chianelli, T.A. Pecoraro, U.S. Patent 4, 528,089 (1985).
[17] R.R. Chianelli, T.A. Pecoraro, U.S. Patent 428822 (1981).
[18] T. Pecoraro, R.R. Chianelli, J. Catal. 67 (1981) 430.
[19] R.R. Chianelli, G. Berhault, Catal. Today 53 (1999) 357.
[20] J.P.R. Vissers, C.K. Groot, E.M. van Oers, V.H.J. de Beer, R. Prins, Bull. Soc. Chim. Belg. 93 (1984) 813.
[21] J.P.R. Vissers, B. Scheeffer, V.H.J. de Beer, J.A. Moulijn, R. Prins, J. Catal. 105 (1987) 277.
[22] P. Afanasiev, G.F. Xia, G. Berhault, B. Jouguet, M. Lacroix, Chem. Mater. 11 (1999) 3216.
[23] M. Soto-Puente, M. Del Valle, E. Flores-Aquino, M. Avalos-Borja, S. Fuentes, J. Cruz-Reyes, Catal. Lett. 113 (2007) 170.
[24] G. Berhault, A. Metha, A.C. Pavel, J. Yang, L. Rendon, M.J. Yacamán, L. Cota Araiza, A. Duarte Moller, R.R. Chianelli, J. Catal. 198 (2001) 9.
[25] G. Alonso, M.H. Siadati, G. Berhault, A. Aguilar, S. Fuentes, R.R. Chianelli, Appl. Catal. A: Gen. 263 (2004) 109.
[26] A. Muller, E.J. Baran, R.O. Carter, Struct. Bond. 26 (1976) 81.
[27] Ch. Calais, N. Matsubayasshi, Ch. Geantet, Y. Yohimura, H. Shimada, A. Nishijima, M. Lacroix, M. Breysse, J. Catal. 174 (1998) 130.
[28] P. Afanasiev, G.F. Xia, B. Jouguet, M. Lacroix, in: A. Corma, F.V. Melo, S. Mendioroz, J.L.G. Fierro (Eds.), Studies in Surface Science and Catalysis, vol. 130, Elsevier Science, 2000, p. 277.
[29] R.R. Chianelli, Int. Rev. Phys. Chem. 2 (1982) 127.
[30] M. Del Valle, J. Cruz-Reyes, M. Avalos-Borja, S. Fuentes, Catal. Lett. 54 (1998) 59.
[31] C. Thiang Tye, K.J. Smith, Catal. Lett. 95 (2004) 203.
[32] I. Bezverkhy, P. Afanasiev, M. Lacroix, Inorg. Chem. 39 (2000) 5416.
[33] J. Cruz-Reyes, M. Avalos-Borja, M.H. Farias, Catal. Lett. 3 (1989) 227.
[34] L. Alvarez, J. Espino, C. Ornelas, J.L. Rico, M.T. Cortez, G. Berhault, G. Alonso, J. Mol. Catal. 210 (2004) 105.
[35] R.R. Chianelli, A.F. Ruppert, M.J. Yacamán, A. Vázquez-Zavala, Catal. Today 23 (1995) 269.
[36] J. Ramirez, R. Cuevas, A. Lopez-Agudo, S. Mendioroz, J.L.G. Fierro, Appl. Catal. 57 (1990) 223.